Available online at www.sciencedirect.com
SCIENCE DIRECT®
Advances in Water Resources 27 (2004) 859–874
Advances in Water Resources
www.elsevier.com/locate/advwatres

Conditional simulations of flow in randomly heterogeneous porous media using a KL-based moment-equation approach

Zhiming Lu [a,*], Dongxiao Zhang [b]

[a] Hydrology, Geochemistry, and Geology Group (EES-6), MS T003, Los Alamos National Laboratory, Los Alamos, NM 87545, USA
[b] Mewbourne School of Petroleum and Geological Engineering, University of Oklahoma, 100 East Boyd, SEC T301, Norman, OK 73019, USA

Received 13 May 2004; received in revised form 9 August 2004; accepted 17 August 2004

Abstract

In this study, we extend the KLME approach, a moment-equation approach based on the Karhunen–Loève decomposition (KL), developed by Zhang and Lu [An efficient, higher-order perturbation approach for flow in randomly heterogeneous porous media via Karhunen–Loève decomposition. J Comput Phys 2004;194(2):773–94] to efficiently incorporate existing direct measurements of the log hydraulic conductivity. We first decompose the conditional log hydraulic conductivity $Y = \ln K_s$ as an infinite series on the basis of a set of orthogonal Gaussian standard random variables $\{\xi_i\}$. The coefficients of this series are related to eigenvalues and eigenfunctions of the conditional covariance function of the log hydraulic conductivity. We then write head as an infinite series whose terms $h^{(n)}$ represent the head contribution at the nth order in terms of σ_Y, the standard deviation of Y, and derive a set of recursive equations for $h^{(n)}$. We assume that $h^{(n)}$ can be expressed as infinite series in terms of the products of n Gaussian random variables. The coefficients in these series are determined by substituting decompositions of Y and $h^{(m)}$, $m < n$, into those recursive equations. We solve the conditional mean head up to fourth-order in σ_Y and the conditional head covariances up to third-order in σ_Y^2. The higher-order corrections for the conditional mean flux and flux covariance can be determined directly from the higher-order moments of the head, using Darcy's law. We compare the results from the KLME approach against those from Monte Carlo (MC) simulations and the conventional first-order moment method. It is evident that the KLME approach with higher-order corrections is superior to the conventional first-order approximations and is computationally more efficient than both the Monte Carlo simulations and the conventional first-order moment method.

Keywords: Karhunen–Loève decomposition; Conditional simulation; Moment equations; Uncertainty; Higher-order correction; Heterogeneity

1. Introduction

Although geological formations are intrinsically deterministic, we usually have incomplete knowledge of their properties. As a result, the medium properties may be treated as random space functions and the equations describing flow and transport in these formations become stochastic. Many predictive models based on the stochastic framework have been developed in the past two decades [4,6,2,25].

Monte Carlo simulations and the moment-equation approach are two widely used methods for solving stochastic partial differential equations. However, both can be computationally expensive for large-scale problems. Zhang and Lu [27] proposed a new approach called the Karhunen–Loève decomposition based moment-equation approach (KLME). The application of the Karhunen–Loève decomposition to solving stochastic boundary value problems has been pioneered by Ghanem and his coauthors [22,8–11]. The essence of

* Corresponding author. Tel.: +1 505 665 2126; fax: +1 505 665 8737.
E-mail address: zhiming@lanl.gov (Z. Lu).

0309-1708/$ - see front matter © 2004 Elsevier Ltd. All rights reserved.
doi:10.1016/j.advwatres.2004.08.001

their technique includes discretizing the independent random process (e.g., log hydraulic conductivity) using the Karhunen–Loève expansion and representing the dependent stochastic process (hydraulic head or concentration) using the polynomial chaos basis. The deterministic coefficients of the dependent process in the polynomial chaos expansion are then calculated via a weighted residual procedure. Roy and Grilli [20] combined the Karhunen–Loève decomposition and the perturbation methods to solve the steady-state flow equation and obtained the mean head to first-order in σ_Y and the head variance to first-order in σ_Y^2. Zhang and Lu [27] evaluated higher-order approximations for the mean and (co)variance of head, on the basis of the Karhunen–Loève decomposition of the stationary process, i.e., log hydraulic conductivity. Specifically, with the combination of the Karhunen–Loève decomposition and perturbation methods, they evaluated the mean head up to fourth-order in σ_Y and the head (co)variance up to third-order in σ_Y^2. They also explored the validity of this approach for different degrees of medium variability and various correlation scales through comparisons against Monte Carlo simulations. Lu and Zhang [18] compared the KLME method with Monte Carlo simulations (MC) and the conventional moment-equation method (CME) in terms of computational efficiency and solution accuracy. They demonstrated that the KLME method is computationally much more efficient than both the Monte Carlo simulations and the conventional moment approach while retaining high accuracy (i.e., close to Monte Carlo results) at least for σ_Y^2 up to 2. However, their results indicated that for strongly heterogeneous media (e.g., $\sigma_Y^2 = 4.0$) the head variance computed from the KLME approach deviates from Monte Carlo results, even though higher-order terms (up to third-order in terms of σ_Y^2) have been included. This motivates us to develop an algorithm to incorporate direct measurements for the reduction of the variability of the log hydraulic conductivity, which may extend the applicable range of the KLME method.

The effects of conditioning on the flow and transport in heterogeneous porous media has been studied by many researchers [3,12,21,19,24,13,14,23,17]. One of the effects of conditioning on measurements of the log hydraulic conductivity is to reduce the overall uncertainty of the log hydraulic conductivity (especially in the vicinity of the conditioning points), which may lead to the reduction of the predictive uncertainties of flow and transport. In addition, conditioning renders the log hydraulic conductivity field statistically inhomogeneous (spatially nonstationary). As a result, the eigenvalues and eigenfunctions of the conditional covariance function may need to be solved numerically, using an algorithm described, for example, in [8]. However, the computational cost of this algorithm is relatively high. At some special cases, for example, two- (or three-) dimensional flow in rectangular (or brick-shaped) domains with a separable exponential unconditional covariance function, the unconditional eigenvalues and eigenfunctions can be solved easily [27], and the conditional eigenvalues and eigenfunctions can be computed readily by taking advantage of the existing unconditional counterparts.

2. Stochastic differential equations

We consider transient water flow in saturated media satisfying the following continuity equation and Darcy's law:

$$S_s \frac{\partial h(\mathbf{x},t)}{\partial t} + \nabla \cdot \mathbf{q}(\mathbf{x},t) = g(\mathbf{x},t), \tag{1}$$

$$\mathbf{q}(\mathbf{x},t) = -K_s(\mathbf{x}) \nabla h(\mathbf{x},t), \tag{2}$$

subject to initial and boundary conditions

$$h(\mathbf{x},0) = H_0(\mathbf{x}), \quad \mathbf{x} \in D, \tag{3}$$

$$h(\mathbf{x},t) = H(\mathbf{x},t), \quad \mathbf{x} \in \Gamma_{\mathrm{D}}, \tag{4}$$

$$\mathbf{q}(\mathbf{x},t) \cdot \mathbf{n}(\mathbf{x}) = Q(\mathbf{x},t), \quad \mathbf{x} \in \Gamma_{\mathrm{N}}, \tag{5}$$

where $\mathbf{q}$ is the flux, $h(\mathbf{x},t)$ is the hydraulic head, $H_0(\mathbf{x})$ is the initial head in the domain D, $H(\mathbf{x},t)$ is the prescribed head on Dirichlet boundary segments Γ_{D}, $K_s(\mathbf{x})$ is the hydraulic conductivity, $Q(\mathbf{x},t)$ is the prescribed flux across Neumann boundary segments Γ_{N}, $\mathbf{n}(\mathbf{x}) = (n_1, \ldots, n_d)^{\mathrm{T}}$ is an outward unit vector normal to the boundary $\Gamma = \Gamma_{\mathrm{D}} \cup \Gamma_{\mathrm{N}}$, and S_s is the specific storage. In this study, we treat $K_s(\mathbf{x})$ as a random space function while S_s as a deterministic constant. Thus, equations (1)–(5) become stochastic partial differential equations. Our aim is to find the conditional mean hydraulic head and mean flux as well as their associated conditional uncertainties.

Though the moment-equation approach is free of assumptions on parameter distributions, for the sake of comparison with the Monte Carlo method, we assume that the hydraulic conductivity $K_s(\mathbf{x})$ follows a log normal distribution, and work with the log-transformed variable $Y(\mathbf{x}) = \ln[K_s(\mathbf{x})] = \langle Y(\mathbf{x}) \rangle + Y'(\mathbf{x})$, where $\langle Y(\mathbf{x}) \rangle$ is the mean and $Y'(\mathbf{x})$ is the zero-mean fluctuation. The conditional mean log saturated hydraulic conductivity $\langle Y(\mathbf{x}) \rangle^{(c)}$, where the superscript (c) stands for conditional quantities, represents a relatively smooth unbiased estimate of the unknown random function $Y(\mathbf{x})$. It may be estimated using standard geostatistical methods, such as kriging, which produces a best linear unbiased estimate that honors measurements and also provides uncertainty measures for the estimate. The log saturated hydraulic conductivity field is conditioned at some measurement points. In turn, the field

is statistically inhomogeneous in that the two-point covariance function $C_Y(\mathbf{x},\mathbf{y})$ depends on the actual locations of two points $\mathbf{x}$ and $\mathbf{y}$ rather than their separation distance. Therefore, the eigenvalues and eigenfunctions of the nonstationary covariance $C_Y(\mathbf{x},\mathbf{y})$, in general, have to be solved numerically.

3. KL decomposition of log hydraulic conductivity

3.1. Unconditional log hydraulic conductivity

For the stochastic process $Y(\mathbf{x},\omega) = \ln[K_s(\mathbf{x},\omega)]$, where $\mathbf{x} \in D$ and $\omega \in \Omega$ (a probability space), because its covariance function $C_Y(\mathbf{x},\mathbf{y}) = \langle Y'(\mathbf{x},\omega)\, Y'(\mathbf{y},\omega)\rangle$ is bounded, symmetric, and positive definite, it can be decomposed into [1]

$$C_Y(\mathbf{x},\mathbf{y}) = \sum_{n=1}^{\infty} \lambda_n f_n(\mathbf{x}) f_n(\mathbf{y}), \tag{6}$$

where λ_n and $f_n(\mathbf{x})$ are called eigenvalues and eigenfunctions, respectively, and $f_n(\mathbf{x})$ are orthogonal and deterministic functions that form a complete set [16]

$$\int_D f_n(\mathbf{x}) f_m(\mathbf{x}) \mathrm{d}\mathbf{x} = \delta_{nm}, \quad n,m \geqslant 1. \tag{7}$$

The mean-removed stochastic process $Y'(\mathbf{x},\omega)$ can be expanded in terms of $f_n(\mathbf{x})$ as

$$Y'(\mathbf{x},\omega) = \sum_{n=1}^{\infty} \xi_n(\omega) \sqrt{\lambda_n} f_n(\mathbf{x}), \tag{8}$$

where $\xi_n(\omega)$ are orthogonal standard Gaussian random variables i.e., $\langle \xi_n(\omega)\rangle = 0$ and $\langle \xi_n(\omega)\ \xi_m(\omega)\rangle = \delta_{nm}$. The expansion in (8) is called the Karhunen–Loève (KL) expansion. For convenience, thereafter, we suppress symbol ω in $Y'(\mathbf{x},\omega)$ and in other dependent functions.

The eigenvalues and eigenfunctions of a covariance function $C_Y(\mathbf{x},\mathbf{y})$ can be solved from the following Fredholm equation

$$\int_D C_Y(\mathbf{x},\mathbf{y}) f(\mathbf{x}) \mathrm{d}\mathbf{x} = \lambda f(\mathbf{y}). \tag{9}$$

For some special types of covariance functions, such as one-dimensional stochastic process with an exponential covariance function $C_Y(x_1,x_2) = \sigma_Y^2 \exp(-|x_1 - x_2|/\eta)$, where σ_Y^2 and η are the variance and the correlation length of the process, respectively, the eigenvalues and eigenfunctions can be solved analytically. For cases of two- (or three-) dimensional flow in rectangular (or brick-shaped) domains with a separable exponential covariance function, such as $C_Y(\mathbf{x},\mathbf{y}) = \sigma_Y^2 \exp(-|x_1 - y_1|/\eta_1 - |x_2 - y_2|/\eta_2)$ for a two-dimensional domain $D = \{(x_1,x_2)\colon\ 0 \leqslant x_1 \leqslant L_1,\ 0 \leqslant x_2 \leqslant L_2\}$, (9) can be solved independently for x_1 and x_2 directions to obtain eigenvalues $\lambda_n^{(1)}$ and $\lambda_n^{(2)}$, and eigenfunctions $f_n^{(1)}(x_1)$ and $f_n^{(2)}(x_2)$. These eigenvalues and eigenfunctions are then combined to form the eigenvalues and eigenfunctions of C_Y [20,27]. The summation of all eigenvalues can be determined by setting $\mathbf{y} = \mathbf{x}$ in (6) and integrating the derived equation with respect to $\mathbf{x}$ over D, i.e., $\sum_{n=1}^{\infty} \lambda_n = \sigma_Y^2\ D$, where D is the area of the flow domain.

In general, however, (9) has to be solved numerically. Ghanem and Spanos [8] presented a Galerkin-type algorithm for solving (9). The basic idea of this algorithm is to choose a complete set of functions $\{\phi_i(\mathbf{x}), i = 1,2,\ldots\}$, express the eigenfunctions f_n as truncated (finite) linear combinations $f_n = \sum_{i=1}^{N} a_{in}\phi_i(\mathbf{x})$, and determine coefficients a_{in} by forcing truncating errors to be orthogonal to $\phi_i(\mathbf{x})$, $i = 1,2,\ldots,N$. This algorithm can be computationally demanding because it requires to evaluate a large number of integrations such as $\int_D\int_D C(\mathbf{x}_1,\mathbf{x}_2)\phi_i(\mathbf{x}_1)\phi_j(\mathbf{x}_2)\mathrm{d}\mathbf{x}_1\,\mathrm{d}\mathbf{x}_2$ and $\int_D \phi_i(\mathbf{x}_1)\phi_j(\mathbf{x}_2)\,\mathrm{d}\mathbf{x}_1\,\mathrm{d}\mathbf{x}_2$. The readers are referred to Ghanem and Spanos [8] for details.

3.2. Conditional log hydraulic conductivity

Suppose we have n_Y measurements $Y_1, Y_2, \ldots, Y_{n_Y}$, located at $\mathbf{x}_1, \mathbf{x}_2, \ldots, \mathbf{x}_{n_Y}$. The conditional mean and covariance of Y can be derived from the kriging technique:

$$\langle Y(\mathbf{x})\rangle^{(c)} = \langle Y(\mathbf{x})\rangle + \sum_{i=1}^{n_Y} \mu_i(\mathbf{x})[Y(\mathbf{x}_i) - \langle Y(\mathbf{x}_i)\rangle], \tag{10}$$

$$C_Y^{(c)}(\mathbf{x},\mathbf{y}) = C_Y(\mathbf{x},\mathbf{y}) - \sum_{i,j=1}^{n_Y} \mu_i(\mathbf{x})\mu_j(\mathbf{y}) C_Y(\mathbf{x}_i,\mathbf{x}_j). \tag{11}$$

The functions $\mu_i(\mathbf{x})$ are weighting functions representing the relative importance of each measurement $Y(\mathbf{x}_i)$ in predicting the value of $\langle Y\rangle^{(c)}$ at location $\mathbf{x}$, and can be solved from the following kriging equations:

$$\sum_{i=1}^{n_Y} \mu_i(\mathbf{x}) C_Y(\mathbf{x}_i,\mathbf{x}_j) = C_Y(\mathbf{x},\mathbf{x}_j), \quad j = 1,2,\ldots,n_Y. \tag{12}$$

Certainly, the covariance function computed from (11) is no longer stationary and the eigenvalues and eigenfunctions corresponding to this nonstationary conditional covariance function have to be solved numerically. They can be obtained using the algorithm described by Ghanem and Spanos [8]. Here we follow Roy and Grilli's [20] algorithm for a special case of a two-dimensional rectangular or three-dimensional brick-shaped domain with an unconditional separable exponential covariance function. We will relate the conditional eigenvalues $\lambda_n^{(c)}$ and eigenfunctions $f_n^{(c)}(\mathbf{x})$ to their corresponding unconditional eigenvalues λ_n and eigenfunctions $f_n(\mathbf{x})$, which can be found easily for unconditional separable covariances [27]. This can be done by linking $\mu_i(\mathbf{x})$ to the eigen quantities of the unconditional covariance C_Y. Since the set of eigenfunctions

$\{f_n\}$ is complete, we can expand $\mu_i(\mathbf{x})$ on the basis of $\{f_n\}$, $\mu_i(\mathbf{x}) = \sum_{k=1}^{\infty} \mu_{ik} f_k(\mathbf{x})$, where μ_{ik} are coefficients to be determined. Substituting this expansion into (12), multiplying $f_m(\mathbf{x})$ on both sides, and integrating the derived equation with respect to $\mathbf{x}$ over D yields

$$\sum_{i=1}^{n_Y} C_Y(\mathbf{x}_i, \mathbf{x}_j)\mu_{im} = \lambda_m f_m(\mathbf{x}_j), \quad j = 1, 2, \ldots, n_Y; \quad m = 1, 2, \ldots \tag{13}$$

If we retain only M terms in approximating the unconditional $Y'(\mathbf{x})$ in (8), the computational effort to obtain all μ_{im} in (13) will be the cost of solving $n_Y \times n_Y$ linear algebraic equations for M times. Note that n_Y, the number of conditioning points on the log hydraulic conductivity, in general is small.

Similar to the unconditional case, the conditional eigenvalues $\lambda_n^{(c)}$ and eigenfunctions $f_n^{(c)}(\mathbf{x})$ of the conditional covariance function $C_Y^{(c)}(\mathbf{x}, \mathbf{y})$ can be solved from the following Fredholm equation:

$$\int_D C_Y^{(c)}(\mathbf{x}, \mathbf{y}) f^{(c)}(\mathbf{x}) d\mathbf{x} = \lambda^{(c)} f^{(c)}(\mathbf{y}). \tag{14}$$

To determine $f^{(c)}$, again we expand it in terms of the unconditional eigenfunctions $f_n(\mathbf{x})$. Writing $f^{(c)}(\mathbf{x}) = \sum_{i=1}^{M} d_i f_i(\mathbf{x})$, substituting this expansion and (11) into (14), multiplying $f_m(\mathbf{y})$ on the derived equation, and integrating it with respect to $\mathbf{y}$ over domain D, one obtains

$$\lambda_m d_m - \sum_{k=1}^{M} \left(\sum_{i,j=1}^{n_Y} C_Y(\mathbf{x}_i, \mathbf{x}_j)\mu_{ik}\mu_{jm} \right) d_k = \lambda^{(c)} d_m, \quad m = 1, 2, \ldots, M, \tag{15}$$

or in a matrix form

$$(\mathbf{A} - \lambda^{(c)}\mathbf{E})\mathbf{d} = 0, \tag{16}$$

where components of $\mathbf{A} = (a_{km})_{M\times M}$, $a_{km} = \lambda_m \delta_{km} - \sum_{i,j=1}^{n_Y} C_Y(\mathbf{x}_i, \mathbf{x}_j)\mu_{ik}\mu_{jm}$, and $\mathbf{E}$ is an $M \times M$ identical matrix. Therefore, the problem of finding the eigenvalues and eigenfunctions of a conditional covariance function $C_Y^{(c)}(\mathbf{x}, \mathbf{y})$ reduces to the problem of finding the eigenvalues and eigenvectors of an $M \times M$ matrix. Because $C_Y(\mathbf{x}_i, \mathbf{x}_j)$ is symmetric, so is matrix $\mathbf{A}$. Note that all M eigenvalues of $\mathbf{A}$ are real and positive. For each eigenvalue $\lambda_n^{(c)}$, the corresponding eigenvector $\mathbf{d_n}$ is then used to construct the eigenfunction corresponding to this eigenvalue, $f_n^{(c)}(\mathbf{x}) = \sum_{i=1}^{M} d_{ni} f_i(\mathbf{x})$. The computational cost of finding conditional eigenvalues and eigenfunctions in this way is much less than that of directly solving them numerically by Galerkin-type techniques. It should be noted, however, that this procedure can be used only if the analytical decomposition of the unconditional covariance function is possible. Otherwise, one has to solve the conditional eigenvalues and eigenfunctions directly from the conditional covariance by solving a Fredholm integral equation numerically.

The Karhunen–Loève decomposition provides an alternative way to generate conditional realizations. Once the conditional eigenvalues $\lambda_n^{(c)}$ and their corresponding eigenfunctions $f_n^{(c)}$ are found, conditional realizations can be generated simply by independently sampling a certain number of values z_n from the standard Gaussian distribution $N(0, 1)$ and then computing $Y'(\mathbf{x}) \approx \sum_{n=1}^{N} z_n \sqrt{\lambda_n^{(c)}} f_n^{(c)}(\mathbf{x})$, where N is the number of terms needed to generate realizations with a given accuracy.

Since eigenvalues $\sqrt{\lambda_n^{(c)}}$ and their corresponding eigenfunctions $f_n^{(c)}(\mathbf{x})$ always come together, in the following derivation, we define new functions $\tilde{f}_n(\mathbf{x}) = \sqrt{\lambda_n^{(c)}} f_n^{(c)}(\mathbf{x})$ and the tilde over f_n is dropped for simplicity.

4. KL-based conditional moment equations

4.1. Conditional head moments

Since the dependent variable $h(\mathbf{x}, t)$ is a function of the input variability σ_Y^2, one may express $h(\mathbf{x}, t)$ as an infinite series as $h(\mathbf{x}, t) = \sum_{m=1}^{\infty} h^{(m)}(\mathbf{x}, t)$. In this series, the order of each term is with respect to σ_Y, the standard deviation of $Y(\mathbf{x})$. We also expand $K_s(\mathbf{x}) = \exp[Y(\mathbf{x})] = \exp[\langle Y(\mathbf{x})\rangle + Y'(\mathbf{x})] = K_G(\mathbf{x})[1 + Y' + (Y')^2/2 + \cdots]$. After combining (1) and (2), substituting expansions of $h(\mathbf{x}, t)$ and $K_s(\mathbf{x})$, and collecting terms at separate order, we obtain

$$\nabla^2 h^{(0)}(\mathbf{x}, t) + \nabla\langle Y(\mathbf{x})\rangle \cdot \nabla h^{(0)}(\mathbf{x}, t) + \frac{g(\mathbf{x}, t)}{K_G(\mathbf{x})} = \frac{S_s}{K_G(\mathbf{x})} \frac{\partial h^{(0)}(\mathbf{x}, t)}{\partial t}, \tag{17}$$

$$h^{(0)}(\mathbf{x}, 0) = H_0(\mathbf{x}), \quad \mathbf{x} \in \Omega, \tag{18}$$

$$h^{(0)}(\mathbf{x}, t) = H_1(\mathbf{x}, t), \quad \mathbf{x} \in \Gamma_D, \tag{19}$$

$$n_i(\mathbf{x}) \frac{\partial h^{(0)}(\mathbf{x}, t)}{\partial x_i} = -Q(\mathbf{x}, t)/K_G(\mathbf{x}), \quad \mathbf{x} \in \Gamma_N \tag{20}$$

and for $m \geqslant 1$

$$\nabla^2 h^{(m)}(\mathbf{x}, t) + \nabla\langle Y(\mathbf{x})\rangle \cdot \nabla h^{(m)}(\mathbf{x}, t) = \frac{S_s}{K_G(\mathbf{x})} \sum_{k=0}^{m} \frac{(-1)^k}{m!} \times [Y'(\mathbf{x})]^k \frac{\partial h^{(m-k)}(\mathbf{x}, t)}{\partial t} - \nabla Y'(\mathbf{x}) \cdot \nabla h^{(m-1)}(\mathbf{x}, t) - \frac{g(\mathbf{x}, t)}{m!\, K_G(\mathbf{x})} [-Y'(\mathbf{x})]^m, \tag{21}$$

$$h^{(m)}(\mathbf{x}, 0) = 0, \quad \mathbf{x} \in D, \tag{22}$$

$$h^{(m)}(\mathbf{x}, t) = 0, \quad \mathbf{x} \in \Gamma_D, \tag{23}$$

$$\nabla h^{(m)}(\mathbf{x},t)\cdot\mathbf{n}(\mathbf{x}) = -\frac{Q(\mathbf{x},t)}{m!\,K_G(\mathbf{x})}[-Y'(\mathbf{x})]^m, \quad \mathbf{x}\in\Gamma_N. \tag{24}$$

Eqs. (17)–(20) are the governing equations for the zeroth-order conditional mean head. In the conventional moment approaches, the higher-order corrections (usually up to second-order) for the conditional mean head are solved from (21)–(24). The first-order (in terms of σ_Y^2) head covariance can be derived from (21)–(24) by setting $m=1$, multiplying the derived equation for $h^{(1)}(\mathbf{x},t)$ by $h^{(1)}(\boldsymbol{\chi},\tau)$, and taking the conditional ensemble mean.

In the KLME approach, we further assume that $h^{(m)}(\mathbf{x},t)$ can be expanded in terms of orthogonal Gaussian random variables ξ_n, $n=1,2,\ldots$

$$h^{(m)}(\mathbf{x},t) = \sum_{i_1,i_2,\ldots,i_m=1}^{\infty}\left(\prod_{j=1}^{m}\xi_{i_j}\right)h^{(m)}_{i_1,i_2,\ldots,i_m}(\mathbf{x},t) \tag{25}$$

for example,

$$h^{(1)} = \sum_{i=1}^{\infty}h_i^{(1)}\xi_i; \quad h^{(2)} = \sum_{i,j=1}^{\infty}h_{ij}^{(2)}\xi_i\xi_j;$$
$$h^{(3)} = \sum_{i,j,k=1}^{\infty}h_{ijk}^{(3)}\xi_i\xi_j\xi_k, \tag{26}$$

where $h^{(m)}_{i_1,i_2,\ldots,i_m}(\mathbf{x},t)$ are deterministic functions to be determined. Substituting the decomposition of $Y'(\mathbf{x})$ and $h^{(m)}(\mathbf{x},t)$ recursively into (21)–(24), we obtain the governing equations for $h^{(m)}_{i_1,i_2,\ldots,i_m}(\mathbf{x},t)$. For example, to determine $h_n^{(1)}(\mathbf{x},t)$, one substitutes the expansion of $Y'(\mathbf{x})$ and $h^{(1)}(\mathbf{x},t)=\sum_{n=1}^{\infty}\xi_n\,h_n^{(1)}(\mathbf{x},t)$ into Eqs. (21)–(24) with $m=1$, uses the orthogonality of set $\{\xi_n\}$, and obtains the governing equations with initial and boundary conditions for $h_n^{(1)}(\mathbf{x},t)$:

$$\nabla^2 h_n^{(1)}(\mathbf{x},t) + \nabla\langle Y(\mathbf{x})\rangle\cdot\nabla h_n^{(1)}(\mathbf{x},t) = \frac{S_s}{K_G(\mathbf{x})}\left[\frac{\partial h_n^{(1)}(\mathbf{x},t)}{\partial t} - f_n(\mathbf{x})\frac{\partial h^{(0)}(\mathbf{x},t)}{\partial t}\right] - \nabla f_n(\mathbf{x})\cdot\nabla h^{(0)}(\mathbf{x}) + \frac{g(\mathbf{x},t)}{K_G(\mathbf{x})}f_n(\mathbf{x}), \tag{27}$$

$$h_n^{(1)}(\mathbf{x},0) = 0, \quad \mathbf{x}\in D, \tag{28}$$

$$h_n^{(1)}(\mathbf{x},t) = 0, \quad \mathbf{x}\in\Gamma_D, \tag{29}$$

$$\nabla h_n^{(1)}(\mathbf{x},t)\cdot\mathbf{n}(\mathbf{x}) = \frac{Q(\mathbf{x},t)}{K_G(\mathbf{x})}f_n(\mathbf{x}), \quad \mathbf{x}\in\Gamma_N. \tag{30}$$

By recalling the definition of $f_n(\mathbf{x})$, it is seen that all driving terms in Eqs. (27)–(30) are proportional to $\sqrt{\lambda_n^{(c)}}$, which decreases as n increases. This ensures that the magnitude of contribution of $h_n^{(1)}(\mathbf{x},t)$ to $h^{(1)}(\mathbf{x},t)$ decreases with n in general. This also clearly indicates that $h_n^{(1)}(\mathbf{x},t)$ are proportional to σ_Y, the standard deviation of the log hydraulic conductivity. Derivation of higher-order terms $h^{(m)}_{i_1,i_2,\ldots,i_m}(\mathbf{x},t)$ for $m>1$ can be found in [27].

We solve $h^{(m)}_{i_1,i_2,\ldots,i_m}(\mathbf{x},t)$ up to fifth-order, i.e., $h^{(0)}(\mathbf{x},t)$, $h_n^{(1)}(\mathbf{x},t)$, $h_{ij}^{(2)}(\mathbf{x},t)$, $h_{ijk}^{(3)}(\mathbf{x},t)$, $h_{ijkl}^{(4)}(\mathbf{x},t)$, and $h_{ijklm}^{(5)}(\mathbf{x},t)$. Once they are solved, we can directly compute the conditional mean head and head covariance without solving equations for the head covariance and the cross-covariance between the log hydraulic conductivity and the head, which are required in the conventional moment-equation approaches. Up to fifth-order in σ_Y, the head is approximated by

$$h(\mathbf{x},t) \approx \sum_{i=0}^{5}h^{(i)}(\mathbf{x},t) \tag{31}$$

which leads to an expression for the conditional mean head

$$\langle h(\mathbf{x},t)\rangle \approx \sum_{i=0}^{5}\langle h^{(i)}(\mathbf{x},t)\rangle = h^{(0)}(\mathbf{x},t) + \sum_{i=1}^{\infty}h_{ii}^{(2)}(\mathbf{x},t) + 3\sum_{i,j=1}^{\infty}h_{iijj}^{(4)}(\mathbf{x},t). \tag{32}$$

It is seen that $\langle h^{(0)}(\mathbf{x},t)\rangle \equiv h^{(0)}(\mathbf{x},t)$ is the conditional mean head solution up to first-order in σ_Y. The second term on the right-hand side of (32) represents the second-order (or third-order) correction to the first-order conditional mean head, and the third term is the fourth-order (or fifth-order) correction. From (31) and (32), one can write the head perturbation up to fifth-order as

$$h'(\mathbf{x},t) = h(\mathbf{x},t) - \langle h(\mathbf{x},t)\rangle \approx \sum_{i=1}^{5}h^{(i)}(\mathbf{x},t) - \langle h^{(2)}(\mathbf{x},t)\rangle - \langle h^{(4)}(\mathbf{x},t)\rangle, \tag{33}$$

where $\langle h^{(2)}\rangle = \langle\sum_{i,j=1}^{\infty}\xi_i\xi_j h_{ij}^{(2)}\rangle = \sum_{i=1}^{\infty}h_{ii}^{(2)}$ and $\langle h^{(4)}\rangle = 3\sum_{i,j=1}^{\infty}h_{iijj}^{(4)}$. This leads to the head variance up to third-order in terms of σ_Y^2 (or, sixth-order in σ_Y)

$$\sigma_h^2(\mathbf{x},t) = \sum_{i=1}^{\infty}[h_i^{(1)}(\mathbf{x},t)]^2 + 2\sum_{i,j=1}^{\infty}[h_{ij}^{(2)}(\mathbf{x},t)]^2 + 6\sum_{i,j=1}^{\infty}h_i^{(1)}(\mathbf{x},t)h_{ijj}^{(3)}(\mathbf{x},t) + \sum_{i,j,k,l,m,n=1}^{\infty}\langle\xi_{ijklmn}\rangle\Big[2h_i^{(1)}(\mathbf{x},t)h_{jklmn}^{(5)}(\mathbf{x},t) + 2h_{ij}^{(2)}(\mathbf{x},t)h_{klmn}^{(4)}(\mathbf{x},t) + h_{ijk}^{(3)}(\mathbf{x},t)h_{lmn}^{(3)}(\mathbf{x},t)\Big] - 2\langle h^{(2)}(\mathbf{x},t)\rangle\langle h^{(4)}(\mathbf{x},t)\rangle. \tag{34}$$

where $\xi_{ijklmn} = \xi_i\xi_j\xi_k\xi_l\xi_m\xi_n$ for convenience. Due to orthoganality of the set $\{\xi_n,\ n=1,2,\ldots\}$, the term $\langle\xi_i\xi_j\xi_k\xi_l\xi_m\xi_n\rangle$ can be evaluated easily by counting the

occurrance of each ξ and using relationships $\langle \xi_i^{2k+1} \rangle = 0$ and $\langle \xi_i^{2k} \rangle = (2k-1)!!$. Here the first term in the right-hand side of (34) represents the head variance up to first-order in σ_Y^2, the second and third terms are second-order (in σ_Y^2) corrections, and the rest terms are the third-order (in σ_Y^2) corrections. The expression for the head covariance can be found in [27].

4.2. Conditional flux moments

Analogous to the head moments, we write $\mathbf{q} = \mathbf{q}^{(0)} + \mathbf{q}^{(1)} + \cdots$, and $\mathbf{q}^{(m)} = \sum \mathbf{q}^{(m)}_{i_1 i_2 \cdots i_m} \xi_1 \xi_2 \cdots \xi_m$. Once we solved head terms $h^{(m)}_{i_1 i_2 \cdots i_m}$, the corresponding flux terms $\mathbf{q}^{(m)}_{i_1 i_2 \cdots i_m}$ can be computed directly from $h^{(m)}_{i_1 i_2 \cdots i_m}$ based on the Darcy's law (see Appendix A). The conditional mean flux up to fourth-order can be written as

$$\begin{aligned} \langle \mathbf{q}(\mathbf{x},t) \rangle &\approx \sum_{i=0}^{5} \langle \mathbf{q}^{(i)}(\mathbf{x},t) \rangle \\ &= \mathbf{q}^{(0)}(\mathbf{x},t) + \sum_{i=1}^{\infty} \mathbf{q}^{(2)}_{ii}(\mathbf{x},t) + 3 \sum_{i,j=1}^{\infty} \mathbf{q}^{(4)}_{iijj}(\mathbf{x},t), \end{aligned} \tag{35}$$

and the conditional flux variance up to third-order in terms of σ_Y^2 is given as

$$\begin{aligned} \sigma^2_{q,s}(\mathbf{x},t) = & \sum_{i=1}^{\infty} [q^{(1)}_{i,s}(\mathbf{x},t)]^2 + 2 \sum_{i,j=1}^{\infty} [q^{(2)}_{ij,s}(\mathbf{x},t)]^2 \\ & + 6 \sum_{i,j=1}^{\infty} q^{(1)}_{i,s}(\mathbf{x},t) q^{(3)}_{ijj,s}(\mathbf{x},t) \\ & + \sum_{i,j,k,l,m,n=1}^{\infty} \langle \xi_{ijklmn} \rangle \Big[2 q^{(1)}_{i,s}(\mathbf{x},t) q^{(5)}_{jklmn,s}(\mathbf{x},t) \\ & + 2 q^{(2)}_{ij,s}(\mathbf{x},t) q^{(4)}_{klmn,s}(\mathbf{x},t) + q^{(3)}_{ijk,s}(\mathbf{x},t) q^{(3)}_{lmn,s}(\mathbf{x},t) \Big] \\ & - 2 \langle q^{(2)}_s(\mathbf{x},t) \rangle \langle q^{(4)}_s(\mathbf{x},t) \rangle, \quad s = 1,2,\ldots,d. \end{aligned} \tag{36}$$

where d is the space dimensionality, subscripts r and s represent the terms corresponding to the rth and sth components of the conditional flux fields.

5. Illustrative examples

In this section, we attempt to examine the validity of the KL-based moment-equation approach in computing higher-order head moments for flow in hypothetical saturated porous media conditional to some direct measurements of the log hydraulic conductivity, by comparing model results with those from Monte Carlo simulations. Meanwhile, we will also demonstrate the effect of conditioning on reducing prediction uncertainties.

We consider a two-dimensional domain in a saturated heterogeneous porous medium (Fig. 1). The flow

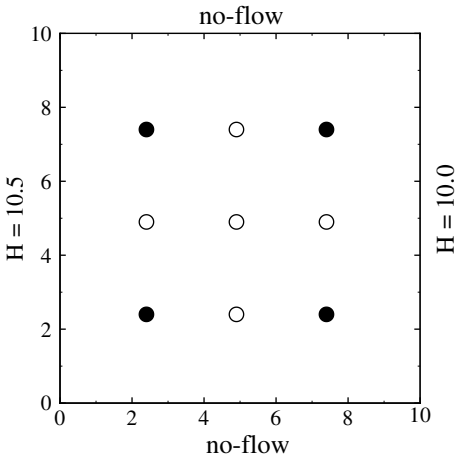

Fig. 1. Problem configuration. Four solid circles are conditioning points for Case 2 and all nine circles are conditioning points for Case 5.

domain is a square of a size $L_1 = L_2 = 10$ [L] (where L is any consistent length unit), uniformly discretized into 40×40 square elements. The no-flow conditions are prescribed at two lateral boundaries. The hydraulic head is prescribed at the left and right boundaries as 10.5 [L] and 10.0 [L], respectively, which produces a mean flow from the left to the right. The unconditional mean of the log hydraulic conductivity is given as $\langle Y \rangle = 0.0$ (i.e., the geometric mean saturated hydraulic conductivity $K_G = 1.0$ [L/T], where T is any consistent time unit). For simplicity, it is assumed in the following examples that the unconditional log saturated hydraulic conductivity $Y(\mathbf{x}) = \ln K_s(\mathbf{x})$ is second-order stationary with a separable exponential covariance function

$$\begin{aligned} C_Y(\mathbf{x},\mathbf{y}) &= C_Y(x_1,x_2;y_1,y_2) \\ &= \sigma_Y^2 \exp\left[-\frac{|x_1 - y_1|}{\eta} - \frac{|x_2 - y_2|}{\eta} \right] \end{aligned} \tag{37}$$

where η is the unconditional correlation scale. In this case, the unconditional eigenvalues λ_n, $n = 1,2,\ldots$, and their corresponding eigenfunctions f_n, $n = 1,2,\ldots$, can be computed analytically [27]. Zhang and Lu [27] discussed the effect of the correlation length on computational costs and solution accuracy. Here we fix $\eta = 4.0$ unless otherwise stated.

To investigate the effect of conditioning, and the accuracy and efficiency of the KLME approach, we design five cases. The first case is a unconditional one with unconditional variance of $\sigma_Y^2 = 2.0$ and a correlation length of $\eta = 4.0$. This case is used for the purpose of illustrating the effect of conditioning by comparing to the second case, where four conditioning points have been added. The locations of these conditioning points are shown in Fig. 1 as solid cycles. The third and fourth cases are respectively similar to Case 1 and Case 2, but with a shorter correlation length $\eta = 2.0$. These two cases are used to investigate the dependence of the effect

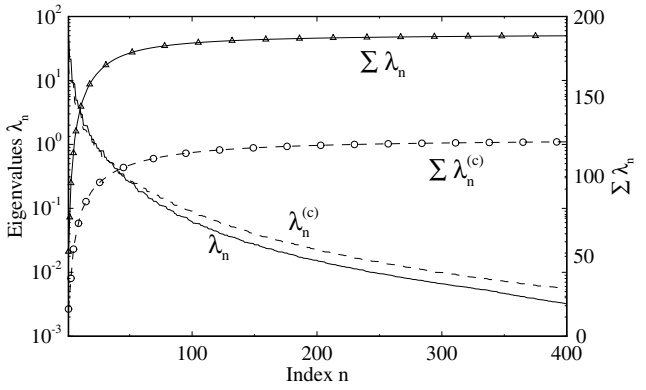

Fig. 2. Unconditional and conditional eigenvalues.

of conditioning on the correlation length. In the fifth case, we modify Case 2 by increasing the variability of Y to $\sigma_Y^2 = 4.0$ and adding five more conditioning points (nine conditioning points in total, see Fig. 1). With such a high variability, Zhang and Lu [27] have showed that, up to third-order in σ_Y^2, the KLME method is not applicable without conditional points.

For the conditional KLME method, we first solve for the unconditional eigenvalues and eigenfunctions. Fig. 2 shows the unconditional eigenvalue λ_n as a function of index n. Also shown in the figure is the accumulative value of the unconditional eigenvalues. Given $\sigma_Y^2 = 2.0$ and the area of flow domain (100 L^2), the accumulative unconditional eigenvalues should be $\sum_{n=1}^{\infty} \lambda_n = \sigma_Y^2 \, D =$ 200.0. It is seen from the figure that the first 100 terms account for about 90% of the total variability. Fig. 3 illustrates some examples of unconditional eigenfunctions. Note that the series of eigenvalues is monotonically decreasing and the characteristic length of the unconditional eigenfunctions f_n is also decreasing as n increases.

Once the unconditional eigenvalues and eigenfunctions are calculated, the conditional eigenvalues and eigenfunctions are computed using the algorithm described in Section 3. The conditional eigenvalues are also shown in Fig. 2. Note that the summation of all conditional eigenvalues is much less than that of the unconditional case, indicating a smaller variability of the conditional Y. Fig. 4 illustrates some of conditional eigenfunctions. Unlike the unconditional eigenfunctions, the characteristic scales of conditional eigenfunctions are not monotonically decreasing as the mode number n increases. We then solve conditional head terms $h^{(m)}$ up to fifth-order and compute the conditional mean head and mean flux up to fourth-order in terms of σ_Y, and the conditional head variance and flux variance up to third-order in terms of σ_Y^2.

For each case, we conduct Monte Carlo simulations. Using the *sgsim* code in GSLIB [15], we first generate a two-dimensional unconditional random field (realization) on a grid of 41×41 nodes, with a specified mean and a covariance function , i.e., (37), and consider this field as a "true" field. The values of this field at conditioning points are taken as "measurements". We then

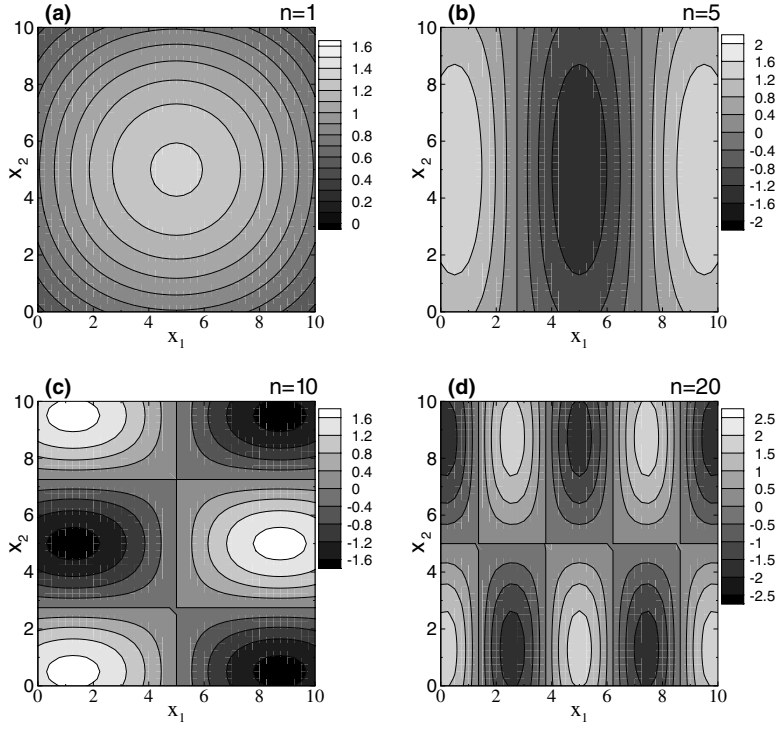

Fig. 3. Examples of unconditional eigenfunctions: (a) $f_1(\mathbf{x})$; (b) $f_5(\mathbf{x})$; (c) $f_{10}(\mathbf{x})$ and (d) $f_{20}(\mathbf{x})$.

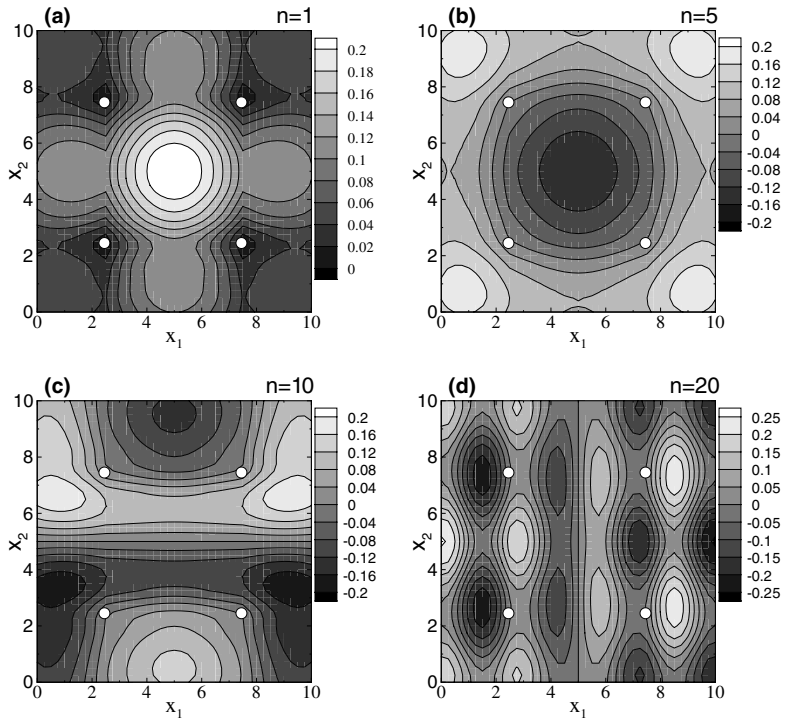

Fig. 4. Examples of conditional eigenfunctions: (a) $f_1^{(c)}(\mathbf{x})$; (b) $f_5^{(c)}(\mathbf{x})$; (c) $f_{10}^{(c)}(\mathbf{x})$ and (d) $f_{20}^{(c)}(\mathbf{x})$.

generate 5000 realizations conditioned on measurement values, again, using *sgsim*. The quality of these conditional realizations is examined by comparing the mean and covariance of the sampled realizations (solid contour lines) with the mean and covariance computed from kriging (dash-dotted lines), as illustrated in Fig. 5. It is seen from the figure that the conditional sample mean and variance resulted from generated realizations are in excellent agreement with those from the kriging method. The steady-state, saturated flow equation is solved for each realization of the log hydraulic conductivity, using the Finite-Element Heat- and Mass-Transfer code (FEHM) by Zyvoloski et al. [28]. Then, the sample statistics of the flow fields, i.e., the conditional mean predictions of head and flux as well as their associated conditional uncertainties (variances), are computed from these realizations. These statistics are considered the "true" solutions that are used to compare against the results from the proposed higher-order conditional KLME approach.

We also compare the results from the KLME approach with those from the conventional first-order moment-equation-based approach (CME) [26], which is applicable to general nonstationary fields, including those resulted from conditioning. The input conditional covariance to the conventional moment method can be

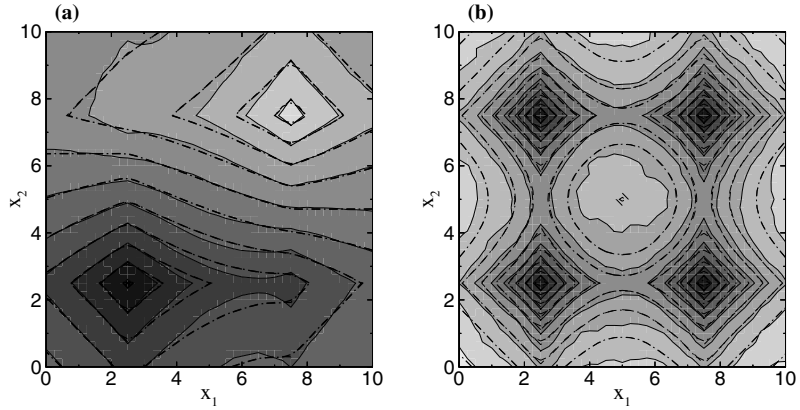

Fig. 5. Comparisons of: (a) conditional mean and (b) conditional variance of the log hydraulic conductivity for Case 2, computed from the Monte Carlo simulations (solid curves) and the kriging method (dashed curves).

computed either from conditional realizations or from the kriging method. It has been verified that the impact of different choices of the input covariance is minimal. As a result, in this study we use the conditional covariance of the log hydraulic conductivity computed from the kriging method as the input covariance for the CME method. In comparing results from the CME and the KLME methods, it is expected that, while the higher-order approximations of the conditional head variance and flux variance from the KLME approach should be close to Monte Carlo results, their first-order approximations shall be almost identical to those from the CME approach, if n_1, the number of terms included in $h^{(1)}$, is sufficiently large. That is to say, the closeness of the first-order variances derived from the conventional moment-equation-based approach and from the KLME approach is an indicator showing if n_1 is large enough.

6. Results and discussions

6.1. Effect of conditioning

The effect of conditioning is twofold. First, conditioning locally reduces the uncertainty of the log hydraulic conductivity around the conditioning points and thus reduces the overall predictive uncertainty of the head and flux. Fig. 6 compares the mean head and the head variance derived from Monte Carlo simulations for Case 1 (solid curves, unconditional) and Case 2 (dashed curves, conditional). Under the given boundary conditions, the mean head for the unconditional case exhibits a linear trend from the left to the right because the log hydraulic conductivity field is statistically homogeneous. For the conditional case, the hydraulic conductivity field is nonstationary and the flow field is no longer uniform. It is seen from the figure that overall the head variance has been significantly reduced, even though there are only four conditioning points in Case 2. The spatial pattern of the head variance distribution for the unconditional case under the given boundary conditions is symmetric with respect to lines $x_1 = 5.0$ and $x_2 = 5.0$. Conditioning distorts such a symmetry. In this example, the head uncertainty in the downstream direction has been considerably reduced while such a reduction of the head uncertainty in the upstream direction is relatively small. This could be ascribed to the spatial distribution of the mean log hydraulic conductivity field (see Fig. 5). Numerical experiments show that the amount of reduction of the head uncertainty is reversed if we rotate the mean log hydraulic conductivity field by 180°. Another important observation from the figure is that conditioning may increase the head variability in some regions, for example in the left-upper corner of Fig. 6(b). However, conditioning does reduce the overall head variability. The average head variability (nodal average) for the unconditional case (Case 1) is 5.43×10^{-3}, comparing to 3.11×10^{-3} for the conditional case (Case 2).

However, such a reduction on the head variability may depend on the correlation length of the log hydraulic conductivity. Intuitively, when the correlation length is large, the region of influence of each individual conditioning point will be large, which leads to relatively large reduction on overall head variability. Fig. 7 compares the mean head and the head variance derived from Monte Carlo simulations for Case 3 and Case 4, where the correlation length has been reduced to $\eta = 2.0$. Comparing to Fig. 6, the reduction on the head variability is not so significant. In fact, the average head variance for the unconditional case (Case 3) is 3.0×10^{-3} and that for the conditional case (Case 4) is 2.84×10^{-3}.

The second effect of the conditioning is that it allows us to apply the KLME method to the cases with a high variability of the unconditional log hydraulic conductivity. Although conditioning may reduce the correlation length of the log hydraulic conductivity, which in turn

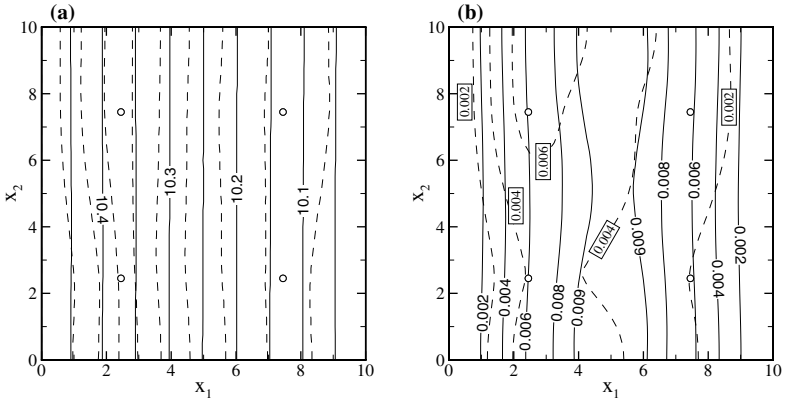

Fig. 6. The unconditional (Case 1, solid curves) and conditional (Case 2, dashed curves) Monte Carlo simulations for: (a) mean head and (b) head variance.

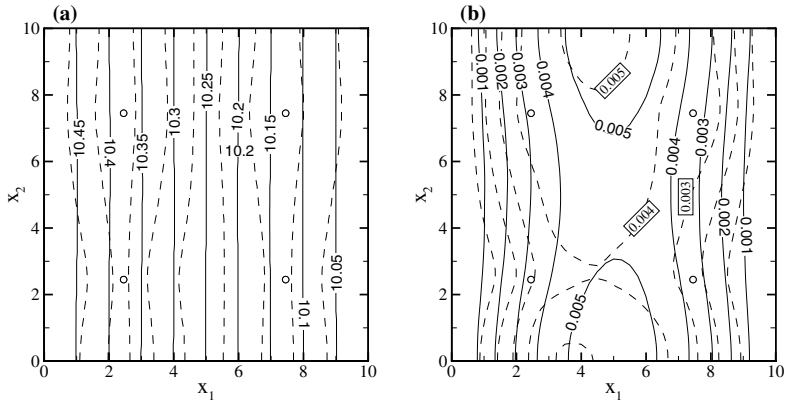

Fig. 7. The unconditional (Case 3, solid curves) and conditional (Case 4, dashed curves) Monte Carlo simulations for: (a) mean head and (b) head variance.

requires more terms to approximate the log hydraulic conductivity in the truncated KL expansion, our numerical examples show that adding a few conditioning points makes it possible to solve the statistical moments for flow in highly heterogeneous media. This will be discussed in detail in the following sections.

6.2. Accuracy of KLME approach

Comparisons of model results from Monte Carlo simulations (MC), the conventional moment-equation approach (CME), and the KLME approach with different orders of approximations for Case 2 are depicted in Figs. 8–11. Fig. 8a shows a contour map comparing the mean head derived from the Monte Carlo simulations and the KLME method with fourth-order in terms of σ_Y, and Fig. 8b compares the head variance from Monte Carlo simulations and the KLME method with a third-order approximation in terms of σ_Y^2. It should be noted that the difference between two quantities plotted in a contour map has been exaggerated and the actual difference is much smaller. The rest of figures show the quantities of interest along the profile $x_2 = 5.0$. It is seen that the mean heads (Fig. 9a) and mean fluxes (Fig. 10) computed from different approaches do not have significant difference due to the particular boundary conditions in our examples. However, the head variance and flux variance derived from various approaches are quite different. Fig. 9b shows that the first-order approximations of the head variance from both CME and KLME are very close, indicating that approximating Y' using 100 terms is adequate for this case. Note that both first-order approximations significantly deviate from the Monte Carlo simulation results, implying that higher-order corrections are needed. When higher-order terms are added, the head variance is getting closer to that from Monte Carlo simulations. In fact, both the second-order and third-order solutions are very close to the Monte Carlo results.

Fig. 11 delivers the similar information. Note that the first-order flux variance from both the CME and the KLME methods are very close and they are only about half of the value derived from Monte Carlo simulations. This strongly suggests that higher-order corrections for the flux covariance be needed for transport simulations, because the particle displacement covariances, which

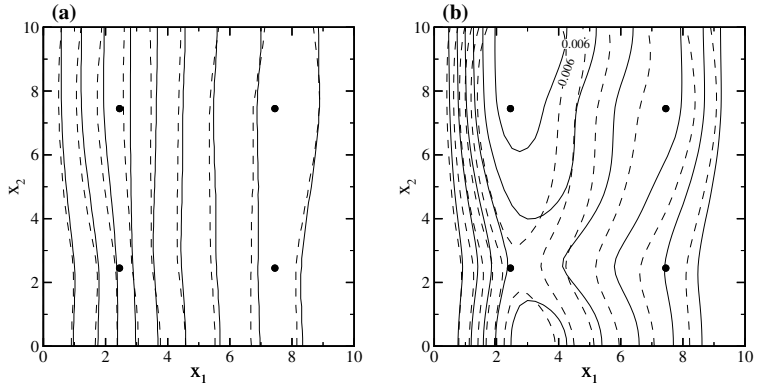

Fig. 8. Comparisons of: (a) the conditional mean head and (b) conditional head variance for Case 2 computed from the MC method (solid curves) and the KLME method to third-order approximation in terms of σ_Y^2 (dashed curves).

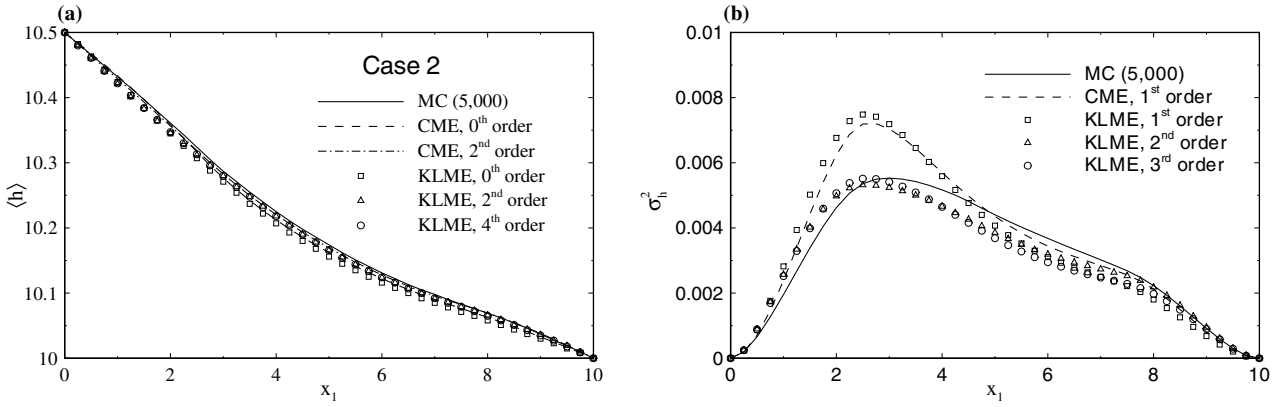

Fig. 9. Comparisons of: (a) the conditional mean head and (b) conditional head variance along the profile $x_2 = 5.0$ for Case 2, computed from the MC method, the CME method, and the KLME method with different orders of approximations.

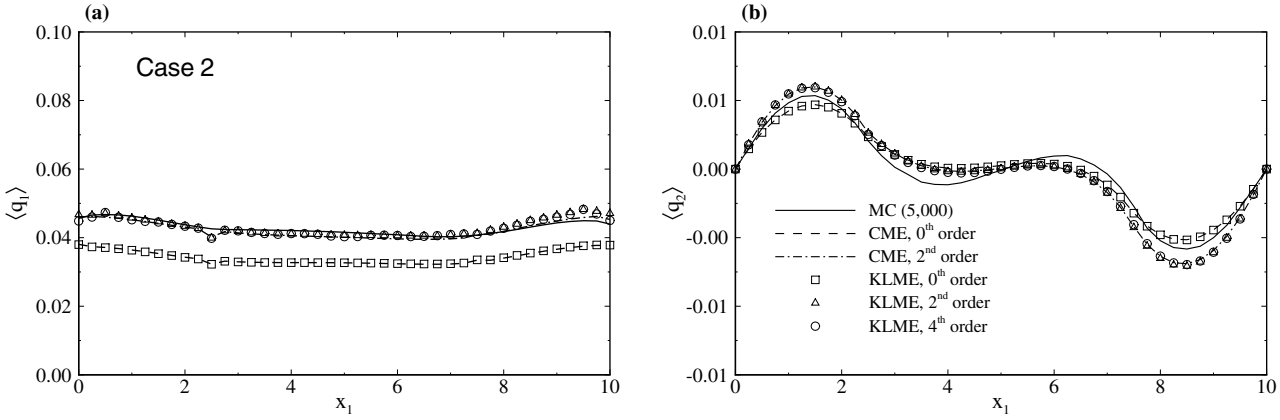

Fig. 10. The conditional mean flux: (a) $\langle q_1 \rangle$ and (b) $\langle q_2 \rangle$ along the profile $x_2 = 5.0$ for Case 2, computed from the MC method, the CME method, and the KLME method with different orders of approximations.

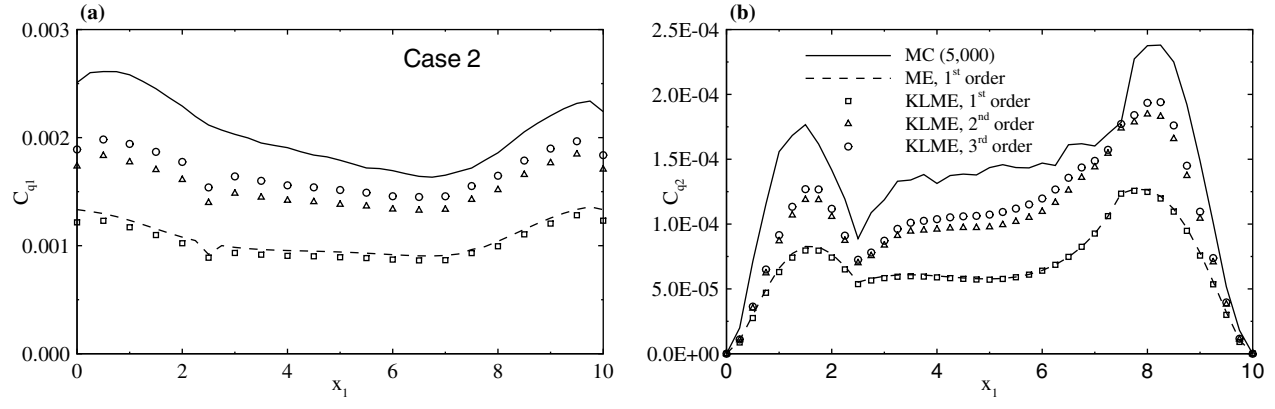

Fig. 11. The conditional flux variance: (a) $\sigma^2_{q_1}$ and (b) $\sigma^2_{q_2}$ along the profile $x_2 = 5.0$ for Case 2, computed from the MC method, the CME method, and the KLME method with different orders of approximations.

describe the spreading of a plume, are highly related to the flux covariance. The figure also demonstrates that adding high-order corrections can significantly improve results. Furthermore, it seems that more terms are required for approximating flux variances than for the head variance.

Figs. 12–15 illustrate such comparisons for Case 5, i.e., the conditional simulation results for a

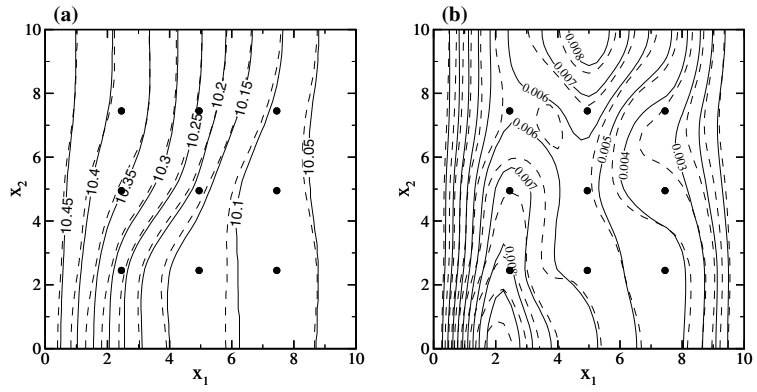

Fig. 12. Comparisons of: (a) the conditional mean head and (b) conditional head variance for Case 5 computed from the MC method (solid curves) and the KLME method to third-order approximation in terms of σ_Y^2 (dashed curves).

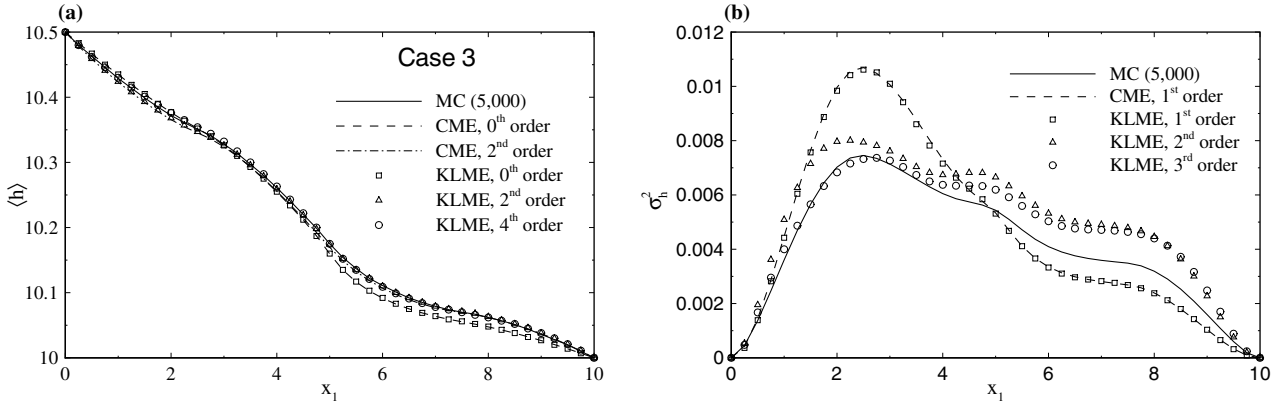

Fig. 13. Comparisons of: (a) the conditional mean head and (b) conditional head variance along the profile $x_2 = 5.0$ for Case 5, computed from the MC method, the CME method, and the KLME method with different orders of approximations.

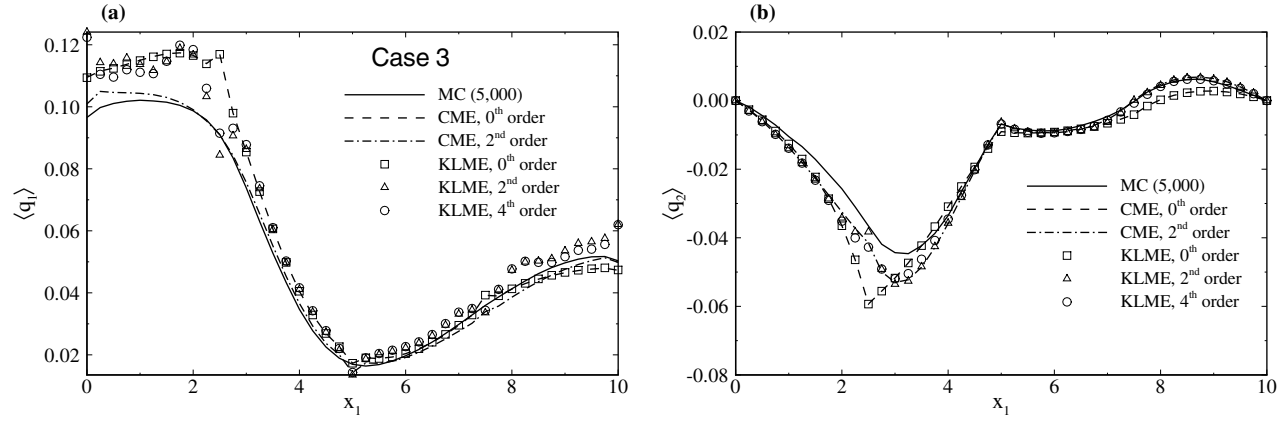

Fig. 14. The conditional mean flux: (a) $\langle q_1 \rangle$ and (b) $\langle q_2 \rangle$ along the profile $x_2 = 5.0$ for Case 5, computed from the MC method, the CME method, and the KLME method with different orders of approximations.

unconditional variance $\sigma_Y^2 = 4.0$. Previous study [27] has shown that, at such a high variability of the log hydraulic conductivity, the unconditional KLME method does not work at least up to third-order in σ_Y^2. By adding only nine conditioning points, the results from the KLME method are getting close to Monte Carlo results. It is shown from Fig. 13b that the first-order approximation of the head variance from both the CME and the

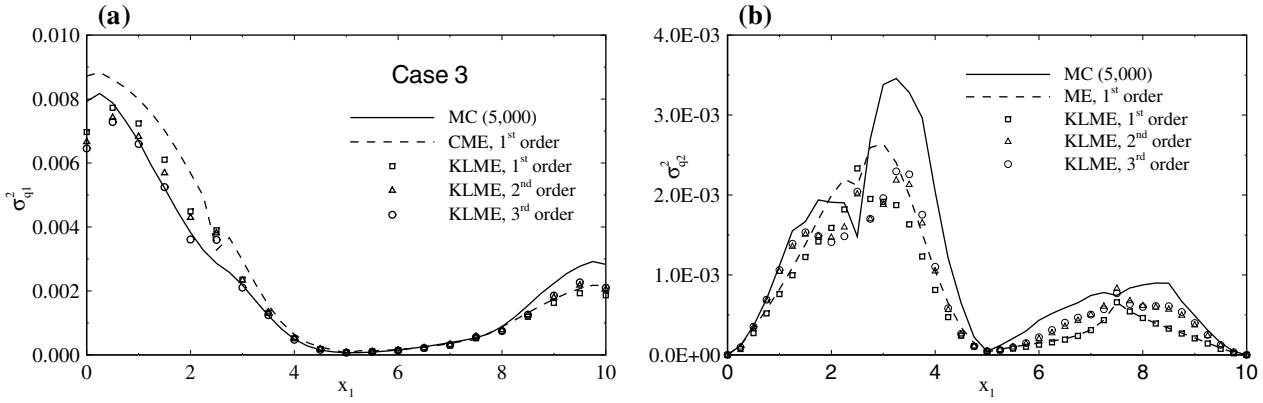

Fig. 15. The conditional flux variance: (a) $\sigma^2_{q_1}$ and (b) $\sigma^2_{q_2}$ along the profile $x_2 = 5.0$ for Case 5, computed from the MC method, the CME method, and the KLME method with different orders of approximations.

KLME methods deviate substantially from the head variance from the Monte Carlo simulations. Including higher-order corrections from the KLEM method improves the results significantly. With nine conditioning points in this case, the flux moments derived from the first-order CME method and from the KLME method with different order of approximations are sufficiently close to these from the Monte Carlo simulations. However, the computational cost for the first-order CME is much higher than that of the KLME method with the first-order approximation, as discussed in detail in the next section.

Fig. 16 compares the mean head and head variance obtained from the Monte Carlo method and the KLME method for Case 4 (the correlation length $\eta = 2.0$), where the profile is taken at $x_2 = 7.5$ (passing two conditioning points). Due to the relatively short correlation length, more terms are required in the truncated KL expansion to approximate the log hydraulic conductivity field. In this case, we retained 1000 terms in the KL expansion, which apparently is adequate by noticing that the first-order approximation of the head variance from the KLME method is almost identical to the results from the first-order CME method. However, both first-order solutions deviate from the Monte Carlo results significantly. By adding higher-order terms in the KLME method, the head variance becomes much closer to the MC results.

6.3. Computational efficiency of the KLME approach

The advantage of the proposed KLME approach largely depends on how many terms are required to approximate $h^{(m)}_{i_1,i_2,\ldots,i_m}$. For Cases 2 and 5 shown above ($\eta = 4.0$), the maximum indices for $h^{(1)}_i$, $h^{(2)}_{ij}$, $h^{(3)}_{ijk}$, $h^{(4)}_{ijkl}$, and $h^{(5)}_{ijklm}$ are 100, 10, 10, 5, and 5, respectively, i.e., index i in $h^{(1)}_i$ running up to 100 and each index in $h^{(2)}_{ij}$ running up to 10, and so on. For instance, the equations

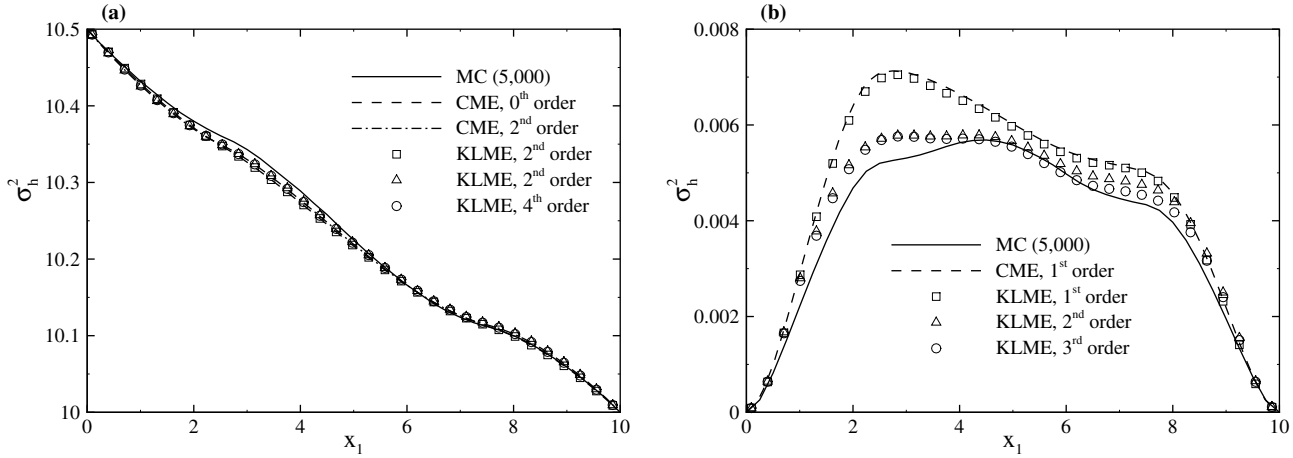

Fig. 16. Comparisons of (a) the conditional mean head, and (b) conditional head variance along the profile $x_2 = 7.5$ for Case 4, computed from the MC method, the CME method, and the KLME method with different orders of approximations.

for term $h_i^{(1)}$, (27)–(30), need to be solved for 100 times, and the equations for $h_{ij}^{(2)}$ need to be solved for 55 times (noting that $h_{ij}^{(2)}$ is symmetric with respect to indices i and j). The total number of times to solve similar equations to obtain $h_i^{(1)}$, $h_{ij}^{(2)}$, $h_{ijk}^{(3)}$, $h_{ijkl}^{(4)}$, and $h_{ijklm}^{(5)}$ will be $100 + 55 + 220 + 70 + 75 = 520$, which is much less than the number of Monte Carlo simulations (at the order of few thousands) required and also less than the number of times for solving the $C_{Yh}(\mathbf{x},\mathbf{y})$ and $C_h(\mathbf{x},\mathbf{y})$ covariance equations ($2N = 3362$, in this case) in the first-order CME approach. For case 4 ($\eta = 2.0$), we have retained 1000 terms in approximating $h^{(1)}$, which increases the computational costs from 520 (in terms of the number of time to solve sets of linear algebraic equations with N unknowns) for Case 2 to 1420, which is still less than computational costs required for the conventional ME method and the MC simulations. In addition, the grid resolution for the KLME method is the same as that for the CME method but can be much coarser than that for the MC simulations. Therefore, the KLME approach (even after including some higher-order terms) could be computationally more efficient than both the first-order CME approach and the MC simulations.

7. Summary and conclusions

Although the moment-equation approach based on the Karhunen–Loève decomposition (KLME) of the unconditional covariance of the log hydraulic conductivity is computationally much more efficient than both the Monte Carlo simulations and the conventional moment-equation method, our previous study demonstrated that the KLME method, up to third-order in σ_Y^2, is not suitable for simulating flow in a medium with extremely strong heterogeneity, for example, $\sigma_Y^2 = 4.0$. In this study, we extended the KLME approach to take advantage of existing direct measurements (conditioning) of the log hydraulic conductivity and developed an algorithm to incorporate such measurements into the unconditional KLME method developed earlier. To incorporate direct measurements, one may compute conditional covariance of the log hydraulic conductivity using, for example, the kriging method and then directly decompose the conditional covariance to calculate the conditional eigenvalues and eigenfunctions corresponding to the conditional covariance, which in general should be solved numerically and involves evaluation of a large number of domain integrations. In the case that the unconditional covariance C_Y is separable, and the flow domain is rectangular (or brick-shaped in three-dimensional cases) the unconditional eigenvalues and eigenfunctions can be derived with relative ease and conditional eigenvalues and eigenfunctions then can be computed from unconditional ones with just a marginal increase in computational costs.

Once the conditional eigenvalues and eigenfunctions have been solved, the exactly same procedure as presented in [27] can be followed: writing the dependent variable, the hydraulic head, as $h = \sum h^{(n)}$, expanding $h^{(n)}$ into a series in terms of the product of n standard Gaussian random variables used in expanding Y, and obtaining sets of equations to determine the deterministic coefficients in these expansions. After these coefficients are solved, the mean head and head covariance can be computed directly without solving any additional equations. Our approach differs from polynomial chaos expansions in that $h^{(n)}$ also satisfies the nth-order moment equations. Higher-order approximations of the flux can be determined from $h_{i_1,i_2,\ldots,i_m}^{(m)}$ using Darcy's law. In this study, we used the conditional KLME method to evaluate the mean quantities (head and flux) to fourth-order in σ_Y and the head (and flux) covariance up to third-order in σ_Y^2. We demonstrated the KLME approach with some examples of steady-state saturated flow in a two-dimensional rectangular domain and compared our results with those from Monte Carlo simulations and from the conventional first-order moment-equation approach.

The moment-equation approach based on the Karhunen–Loève decomposition (KLME) allows us to evaluate higher-order flow moments with relatively small computational efforts. To first-order in the variance of the log hydraulic conductivity (i.e., σ_Y^2), the conditional KLME approach gives results that are consistent with those by the conventional moment-equation approach (CME). Owing to the rapid convergence of the first-order head term, i.e., expansion (25), the first-order KLME approach is generally much more efficient than the CME approach for the cases considered in this study. When the variability of the log hydraulic conductivity is relatively large, first-order approximations are not accurate enough and high-order corrections are needed. These higher-order corrections can be derived from the KLME method with relatively small computational costs.

When the porous media are strongly heterogeneous, say $\sigma_Y^2 = 4.0$, it has been shown [27] that the results from the KLME method deviate significantly from Monte Carlo results, even if up to third-order corrections have been included. However, incorporating a few direct measurements of the log hydraulic conductivity renders the KLME method applicable. Conditioning not only reduces the overall predictive uncertainty, but also extends the applicable range of the KLME approach to highly heterogeneous media.

The effect of conditioning depends on the number of conditioning points and their spatial distribution. In addition, the correlation length also has some impact on the effect of conditioning. For cases with a relatively large correlation length, the reduction on the overall predictive uncertainty will be more significant.

Acknowledgment

This study was supported by DOE/NGOTP under contract AC1005000.

Appendix A

Writing $\mathbf{q}(\mathbf{x},t)=\mathbf{q}^{(0)}+\mathbf{q}^{(1)}+\cdots$, $h(\mathbf{x},t)=h^{(0)}+h^{(1)}+\cdots$, and $K_s(\mathbf{x})=K_G[1+Y'+\cdots]$, substituting these expressions into equation (2), and collecting terms at separate order yields a general form

$$\mathbf{q}^{(n)}(\mathbf{x},t)=-K_G(\mathbf{x})\sum_{k=0}^{n}\frac{[Y'(\mathbf{x})]^k}{k!}\nabla h^{(n-k)}(\mathbf{x},t) \tag{A.1}$$

Substituting decompositions of $Y'(\mathbf{x})$ and $h^{(i)}(\mathbf{x},t)$, $i=\overline{1,n}$, into (A.1) and taking its expectation, we have

$$\begin{aligned}\mathbf{q}^{(n)}(\mathbf{x},t)&=-K_G(\mathbf{x})\sum_{i_1,i_2,\ldots,i_n=1}^{\infty}\xi_{i_1}\xi_{i_2}\ldots\xi_{i_n}\\&\quad\times\sum_{k=0}^{n}\frac{1}{k!}\left(\prod_{j=1}^{k}f_{i_j}(\mathbf{x})\right)\nabla h^{(n-k)}_{i_{k+1},\ldots,i_n}(\mathbf{x},t)\\&=\sum_{i_1,i_2,\ldots,i_n=1}^{\infty}\xi_{i_1}\xi_{i_2}\ldots\xi_{i_n}\mathbf{q}^{(n)}_{i_1,i_2,\ldots,i_n}\end{aligned} \tag{A.2}$$

To make $\mathbf{q}^{(n)}_{i_1,i_2,\ldots,i_n}$ symmetric with respect to its indexes, we write it as

$$\begin{aligned}\mathbf{q}^{(n)}_{i_1,i_2,\ldots,i_n}(\mathbf{x},t)&=-K_G(\mathbf{x})\sum_{k=0}^{n}\frac{(n-k)!}{n!}\\&\quad\times\sum_{P_{i_1,i_2,\ldots,i_n}}\left(\prod_{j=1}^{k}f_{i_j}(\mathbf{x})\right)\nabla h^{(n-k)}_{i_{k+1},\ldots,i_n}(\mathbf{x},t)\end{aligned} \tag{A.3}$$

For example,

$$\mathbf{q}^{(0)}(\mathbf{x},t)=-K_G(\mathbf{x})\nabla h^{(0)}(\mathbf{x},t), \tag{A.4}$$

$$\mathbf{q}^{(1)}_i(\mathbf{x},t)=-K_G(\mathbf{x})[\nabla h^{(1)}_i(\mathbf{x},t)+f_i\nabla h^{(0)}(\mathbf{x},t)], \tag{A.5}$$

$$\begin{aligned}\mathbf{q}^{(2)}_{ij}(\mathbf{x},t)&=-K_G(\mathbf{x})\left[\nabla h^{(2)}_{ij}(\mathbf{x},t)+\frac{1}{2}f_i\nabla h^{(1)}_j(\mathbf{x},t)\right.\\&\quad\left.+\frac{1}{2}f_j\nabla h^{(1)}_i(\mathbf{x},t)+\frac{1}{2}f_if_j\nabla h^{(0)}(\mathbf{x},t)\right]\end{aligned} \tag{A.6}$$

and so on where second summation is over a subset of the permutations of $\{i_1,i_2,\ldots,i_n\}$, in which repeated terms are excluded. Because of normality and orthogonality of the set $\{\xi_i,\ i=1,2,\cdots\}$, it is easy to see that $\langle\xi_{i_1}\xi_{i_2}\cdots\xi_{i_n}\rangle\equiv 0$ for odd n, and from (A.2) we have $\langle\mathbf{q}^{(n)}(\mathbf{x},t)\rangle\equiv 0$ for odd n. For even n, $\langle\mathbf{q}^{(n)}(\mathbf{x},t)\rangle$ can be evaluated in a way similar to evaluation of mean head. Up to fifth-order in σ_Y, the flux is approximated as

$$\mathbf{q}(\mathbf{x},t)\approx\sum_{i=0}^{5}\mathbf{q}^{(i)}(\mathbf{x},t) \tag{A.7}$$

which leads to an expression for mean flux

$$\begin{aligned}\langle\mathbf{q}(\mathbf{x},t)\rangle&\approx\sum_{i=0}^{5}\langle\mathbf{q}^{(i)}(\mathbf{x},t)\rangle\\&=\mathbf{q}^{(0)}(\mathbf{x},t)+\sum_{i=1}^{\infty}\mathbf{q}^{(2)}_{ii}(\mathbf{x},t)+3\sum_{i,j=1}^{\infty}\mathbf{q}^{(4)}_{iijj}(\mathbf{x},t).\end{aligned} \tag{A.8}$$

From Eqs. (A.7) and (A.8) one obtains the perturbation of flux up to fifth-order

$$\begin{aligned}\mathbf{q}'(\mathbf{x},t)&\approx\mathbf{q}(\mathbf{x},t)-\langle\mathbf{q}(\mathbf{x},t)\rangle\\&=\sum_{i=1}^{5}\mathbf{q}^{(i)}(\mathbf{x},t)-\langle\mathbf{q}^{(2)}(\mathbf{x},t)\rangle-\langle\mathbf{q}^{(4)}(\mathbf{x},t)\rangle,\end{aligned} \tag{A.9}$$

where $\langle\mathbf{q}^{(2)}\rangle=\sum_{i=1}^{\infty}\mathbf{q}^{(2)}_{ii}$ and $\langle\mathbf{q}^{(4)}\rangle=3\sum_{i,j=1}^{\infty}\mathbf{q}^{(4)}_{iijj}$. Eq. (A.9) together with (A.2) leads directly to (36).

References

[1] Courant R, Hilbert D. Methods of mathematical physics. Interscience: New York; 1953.
[2] Cushman JH. The physics of fluids in hierarchical porous media: Angstroms to miles. Norwell, MA: Kluwer Academic Publishers; 1997.
[3] Dagan G. Stochastic modeling of groundwater flow by unconditional and conditional probabilities: 1. Conditional simulation and the direct problem. Water Resour Res 1982;18(4):813–33.
[4] Dagan G. Flow and transport in porous formations. New York: Springer-Verlag; 1989.
[6] Gelhar LW. Stochastic subsurface hydrology. Englewood Cliffs, NJ: Prentice-Hall; 1993.
[8] Ghanem R, Spanos PD. Stochastic finite elements: a spectral approach. Springer-Verlag: New York; 1991.
[9] Ghanem R, Kruger RM. Numerical solution of spectral stochastic finite element systems. Comput Methods Appl Mech Engrg 1996;129:289–303.
[10] Ghanem R. Scale of fluctuation and the propagation of uncertainty in random porous media. Water Resour Res 1998;34(9):2123–36.
[11] Ghanem R. Probabilistic characterization of transport in heterogeneous media. Comput Methods Appl Mech Engrg 1998;158:199–220.
[12] Graham WD, McLaughlin D. Stochastic analysis of nonstationary subsurface solute transport, 2. Conditional moments. Water Resour Res 1989;25(11):2331–55.
[13] Guadagnini A, Neuman SP. Nonlocal and localized analyses of conditional mean steady-state flow in bounded, randomly nonuniform domains: 1. Theory and computational approach. Water Resour Res 1999;35(10):2999–3018.
[14] Guadagnini A, Neuman SP. Nonlocal and localized analyses of conditional mean steady-state flow in bounded, randomly nonuniform domains: 2. Computational examples. Water Resour Res 1999;35(10):3019–39.
[15] Deutsch CV, Journel AG. GSLIB: geostatistical software library. New York: Oxford Univ. Press; 1998.
[16] Loeve M. Probability theory. Fourth ed. Berlin: Springer-Verlag; 1977.
[17] Lu Z, Neuman SP, Guadagnini A, Tartakovsky DM. Conditional moment analysis of steady-state unsaturated flow in bounded,

randomly heterogeneous soils. Water Resour Res 2002;38(4). 10.1029/2001WR000278.
[18] Lu Z, Zhang D. A comparative study on quantifying uncertainty of flow in heterogeneous media using Monte Carlo simulations, the conventional and the KL-based moment-equation approaches. SIAM J. Scient Comput [in press].
[19] Neuman SP. Eulerian–Lagrangian theory of transport in space–time nonstationary velocity fields: exact nonlocal formalism by conditional moments and weak approximations. Water Resour Res 1993;29(3):633–45.
[20] Roy RV, Grilli ST. Probabilistic analysis of the flow in random porous media by stochastic boundary elements. Eng Anal Bound Elem 1997;19:239–55.
[21] Rubin Y. Prediction of tracer plume migration in disordered porous media by the method of conditional probabilities. Water Resour Res 1991;27(6):1291–308.
[22] Spanos P, Ghanem R. Stochastic finite element expansion for random media. J Eng Mech ASCE 1989;115(5):1035–53.
[23] Tartakovsky DM, Neuman SP, Lu Z. Conditional stochastic averaging of steady-state unsaturated flow by means of Kirchhoff transformation. Water Resour Res 1999;35(3):731–45.
[24] Zhang D, Neuman SP. Eulerian–Lagrangian analysis of transport conditioned on hydraulic data, 1, Analytical–numerical approach. Water Resour Res 1995;31(1):39–51.
[25] Zhang D. Stochastic methods for flow in porous media: coping with uncertainties. San Diego, CA: Academic Press; 2002.
[26] Zhang D, Lu Z. Stochastic analysis of flow in a heterogeneous unsaturated-saturated system. Water Resour Res 2002;38(2). 10.1029/2001WR000515.
[27] Zhang D, Lu Z. An efficient, higher-order perturbation approach for flow in randomly heterogeneous porous media via Karhunen–Loeve decomposition. J Comput Phys 2004;194(2):773–94.
[28] Zyvoloski GA, Robinson BA, Dash ZV, Trease LL. Summary of the models and methods for the FEHM application–A Finite-Element Heat- and Mass-Transfer code. LA-13307-MS, Los Alamos National Laboratory; 1997.